TU Delft

Delft University of Technology

Bayesian Inference of Aircraft Initial Mass

Sun, Junzi; Ellerbroek, Joost; Hoekstra, Jacco

Publication date
2017

Document Version
Final published version

Published in
12th Seminar Papers

Citation (APA)
Sun, J., Ellerbroek, J., & Hoekstra, J. (2017). Bayesian Inference of Aircraft Initial Mass. In *12th Seminar Papers: 12th USA/Europe Air Traffic Management Research and Development Seminar*

Important note
To cite this publication, please use the final published version (if applicable).
Please check the document version above.

Copyright
Other than for strictly personal use, it is not permitted to download, forward or distribute the text or part of it, without the consent of the author(s) and/or copyright holder(s), unless the work is under an open content license such as Creative Commons.

Takedown policy
Please contact us and provide details if you believe this document breaches copyrights.
We will remove access to the work immediately and investigate your claim.

This work is downloaded from Delft University of Technology.
For technical reasons the number of authors shown on this cover page is limited to a maximum of 10.

Twelfth USA/Europe Air Traffic Management Research and Development Seminar (ATM2017)

Bayesian Inference of Aircraft Initial Mass

Junzi Sun, Joost Ellerbroek, Jacco Hoekstra
Control and Simulation, Faculty of Aerospace Engineering
Delft University of Technology
Delft, The Netherlands

***Abstract*—Aircraft mass is a crucial piece of information for studies on aircraft performance, trajectory prediction, and many other ATM topics. However, it is a common challenge for researchers who have no access to this proprietary information. Previously, several studies have proposed methods to estimates aircraft weight, most of which are focused on specific parts of the flight. Often due to inaccurate input data or biased assumptions, a significant number of estimates can result outside of the weight limitation boundaries. This paper proposes an approach that makes use of multiple observations to get a better estimate for a complete flight. By looking at flight data from a complete trajectory and calculating aircraft mass at different flight phases based on different methods, together with fuel flow models, multiple observations of aircraft initial mass can then be derived. Using the Bayesian inference method, final estimates can be made with a higher level of confidence.**

Keywords - aircraft mass, weight estimation, Bayesian inference

NOMENCLATURE

TO / to	Aircraft takeoff phase
IC / ic	Aircraft initial climb phase
CL / cl	Aircraft climb phase
CR / cr	Aircraft cruise phase
DE / de	Aircraft descent phase
FA / fa	Aircraft final approach phase
LD / ld	Aircraft landing phase

I. INTRODUCTION

Aircraft mass is one of the most important parameters when studying aircraft performance. However, data concerning the mass of almost all modern commercial flights are treated as confidential information by airliners. Within the research community, a few methods have been developed in order to estimate such parameters based on flight data, either from radar data or more recently from ADS-B data.

Sun et al., for instance, use ADS-B data from takeoff to estimate the initial mass of an aircraft with two different analytical methods [1]. Two other studies by Alligier et al. developed least square and machine learning methods, with a focus on the climbing phase of aircraft [2], [3]. In a similar approach considering climbing aircraft, Schultz et al. implemented an adaptive estimation method for mass and thrust approximation [4]. On the operational side, a different approach tried to calculate weight of an aircraft based on approximation of each weight component, i.e. aircraft empty weight, fuel weight, and payload weight [5]. However, despite the limitation on using data from only certain parts of the trajectory, it is not possible to be certain of any individual estimates. One can only conclude the possible distribution of aircraft mass based on a great number of flights.

In flight, aircraft mass varies as a function of fuel flow. Several studies have been conducted to estimate fuel burn. Methods have been proposed that are based on radar track data [6], as well as a classification model from the Flight Data Recorder [7]. Other fuel flow calculation models obtained from empirical data can be found in BADA [8] and the ICAO engine emission databank [9], which are used for this paper due their simplicity and accessibility.

In this paper, several of the above approaches are combined with new mass estimation methods at different phases of flight. Independently, different mass estimates will first be calculated with appropriate methods for each flight phase. Then, a Bayesian inference approach is established to use these calculations as independent measurements, combining a priori knowledge of initial aircraft mass probability distribution to produce the maximum a posteriori estimations. The advantage of the Bayesian approach is that it takes into account prior probability distribution and physical limitations of possible aircraft mass, and it is able to produce an estimate for any given flight based on flight data with the knowledge of aircraft type.

The remainder of the paper is structured as follows. Section two describes all six different mass computation methods based on data from different flight phases. Section three presents the Bayesian inference method process and a close-form solution for normally distributed priors. Section four discusses the results for several aircraft types and parameter sensitivities. Finally, discussion and conclusions are presented in sections five and six.

II. INITIAL MASS COMPUTATIONS

This section describes several methods that can be used independently to compute aircraft mass at different flight phases. The total energy model (TEM), shown in Equation 1, is used in most of the methods. In addition, BADA3 aerodynamic coefficients are used to calculate the thrust and drag in some of the phases when applicable [8].

$$\begin{aligned} (T-D)\cdot V &= m\cdot a\cdot V + m\cdot g\cdot V_h \\ D &= \frac{1}{2}\rho V^2 S\cdot C_D \\ L &= \frac{1}{2}\rho V^2 S\cdot C_L \\ C_D &= C_{D0} + KC_L^2 \end{aligned} \tag{1}$$

Here, T and D are the thrust and drag of the aircraft, V, a, and V_h are the horizontal airspeed, acceleration, and vertical speed respectively. C_D, C_L, C_{D0}, and K are coefficients for drag, lift, zero drag, and induced drag. ρ and S are the air density and the aircraft wing surface.

With the complete flight trajectory based on the total energy model, mass can be computed at several phases (ie.: takeoff, climb, descent, approach, and landing), as illustrated in Figure 1. These values will be used as independent measurements for further Bayesian inference. A fuel flow model also needs to be considered to derive the initial mass at takeoff.

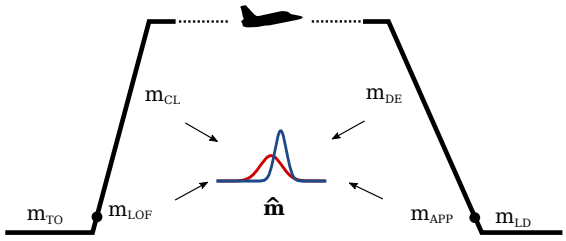

Fig. 1. Bayesian inference diagram

A. Taking off

While an aircraft is on the runway before liftoff, there is only horizontal acceleration. However, in addition to the aerodynamic drag, ground friction also needs to be considered, which is proportional to the normal force on the ground. The friction coefficient is denoted by μ_1. A common value is around 0.02 for concrete runways [10]. Equation 1 then can be re-written as follows:

$$T - D - D_g = ma \tag{2}$$
$$D_g = \mu_1(W - L) \tag{3}$$

Due to the fact that BADA (version 3) does not have an accurate thrust model for the ground phase at takeoff, thrust needs to be computed with other models. Alternatively, the maximum takeoff thrust can be calculated from empirical data using a second-degree polynomial model [11]. This approach provides a fairly good approximation of thrust for two-shaft turbofan engines. This simplified model can also later be used during other phases of flight. The maximum takeoff thrust can be expressed as a function of velocity:

$$T_{max} = f(V) = T_\infty(1 + c_1V + c_2V^2) \tag{4}$$

where T_∞ is the maximum static thrust at zero speed. c_1 and c_2 are coefficients obtained from empirical data fitting. When the requirement of minimum excess thrust is satisfied, aircraft can take off with reduced thrust. This has become common practice for airliners to extend engine life and reduce costs. To accommodate this possibility in the model, a thrust coefficient η is introduced that satisfies $\eta \leq 1$. Equation 2 can be rewritten as:

$$\eta T_{max} - (\mu_1 g + a)m - \tfrac{1}{2}\rho V^2 S(C_D - \mu_1 C_L) = 0 \tag{5}$$

It is also common practice that under the available thrust, takeoffs aim to minimize the takeoff length, where the total drags are at minimal. Hence the optimized lift coefficient can be calculated as follows:

$$C_L = \frac{\mu_1}{2K_{to}} \tag{6}$$

The mass of an aircraft is then calculated discretely at each sample point:

$$\eta T_{max} - (\mu_1 g + a)m - \tfrac{1}{2}\rho V^2 S(C_{D0,to} - \frac{\mu_1^2}{4K_{to}}) = 0 \tag{7}$$

Let the left part of the equation be $\boldsymbol{f}_1(m, \eta)$. The task is to find the optimal $\hat{m}$ and $\hat{\eta}$ that minimize the squared sum of $\boldsymbol{f}_1$ of all takeoff data samples. The solution can be found as follows, with constraints on m and η.

$$\begin{aligned} \hat{m}, \hat{\eta} &= \arg\min_{m,\eta} \sum_{i=1}^{N} \boldsymbol{f}_1^2(m, \eta) \\ m &\in [0,\ 2 \times m_{mtw}] \\ \eta &\in [0.8, 1] \end{aligned} \tag{8}$$

B. Liftoff and approach speed

At each takeoff and approach, optimal speeds are usually selected, which are correlated to the stall speed. Even though it is a relatively weaker correlation at takeoff, both speeds can be used as indicators to infer aircraft mass.

This method first observes the aircraft speed at the moment of liftoff and approach. Then it infers the mass taking into account the relationship with stall speed at maximum takeoff or landing weight when it is available from the aircraft manufacturer. When these parameters are not available, BADA reference data are used.

According to FAA Federal Aviation Regulations, at takeoff, the speed of an aircraft is at least 20% over the stall speed. Assuming lift and weight are the same at liftoff, the following relation can be derived under certain assumptions:

$$\begin{aligned} W_{to} = L_{to} \quad &\Rightarrow \quad m_{to}g = \frac{1}{2}\rho S C_L V_{lof}^2 \\ &\Rightarrow \quad m_{to} \propto V_{lof}^2 \end{aligned} \tag{9}$$

where the takeoff mass is proportional to the liftoff speed squared, under the assumptions of the same aircraft model and lift configurations. Knowing reference weight and its stall speed (V_S), it is possible to calculate such a constant coefficient:

$$C = \frac{m_{to}}{V_{lof}^2} \tag{10}$$
$$= \frac{m_{ref,lof}}{V_{ref,lof}^2} \leq \frac{m_{ref,lof}}{1.2^2 \cdot V_{S,ref,lof}^2} \tag{11}$$

Then at any given observed takeoff, the initial mass can be approximated using the following equation:

$$m_{to} \approx \left(\frac{m_{ref,lof}}{1.2^2 \cdot V_{S,ref,lof}^2} \right) V_{lof}^2 \tag{12}$$

A similar relationship can also be obtained at landing. The approach speed empirically is around 30% over the stall speed. The landing mass then can be approximated as follows:

$$m_{ld} \approx \left(\frac{m_{ref,app}}{1.3^2 \cdot V_{S,ref,app}^2} \right) V_{app}^2 \tag{13}$$

C. Climb and descent phase

During the climb and descent phases, data (horizontal speed and climb/descent rate) can be observed. Assuming standard atmospheric conditions, the total energy model in Equation 1 can be expanded at each time step as follows:

$$\begin{aligned}
(T_i - D_t)\ V_i &= m_i a_i V_i + m_i g V_{hi} && (14)\\
m_i &= m_0 + m_{i,fuel} && (15)\\
T_i &= \eta T_{max,i} \ = \ \eta f(h_i, V_i) && (16)\\
D_i &= \frac{1}{2} C_D \rho_i V_i^2 S && (17)\\
L_i &= m_i g \cos(\gamma_i) \ = \ \frac{1}{2} C_{L,i} \rho_i V_i^2 S && (18)\\
C_D &= C_{D0} + K C_{L,i}^2 && (19)
\end{aligned}$$

where γ represents the path angle. Maximum thrust profile T_{max} is a function of pressure altitude and airspeed and η is an assumed thrust coefficient for the entire climb or descent, describing the actual thrust setting as a percentage of maximum thrust.

Given all observed and known variables, the above equations can be rewritten into the follow equation:

$$\begin{aligned}
&\frac{2Kg^2 \cos^2(\gamma_i)}{\rho_i V_i^2 S} \cdot m_i^2 + \left(a_i + g \frac{V_{hi}}{V_i} \right) \cdot m_i \\
&\quad + \frac{1}{2} C_{D0} \rho_i V_i^2 S - \eta \cdot T_{max,i} = 0
\end{aligned} \tag{20}$$

Fuel consumption can be estimated according to Section II-E where the last remaining two unknown variables m_0 and η are to be found.

This process is similar to the takeoff method but includes more parameters in the equation. Let the left side of Equation 20 be $\boldsymbol{f}_2(m, \eta)$. The task is to find the optimal $\hat{m}$ and $\hat{\eta}$ that minimize the squared sum of $\boldsymbol{f}_2$ of all N data samples. The mass is constrained by the aircraft Operational Empty Weight and the Maximum Takeoff Weight, and thrust reduction is no larger than 20% of the maximum thrust profile. The solution can be found as follows for climbing flights:

$$\begin{aligned}
\hat{m}_0, \hat{\eta} &= \arg\min_{m_0, \eta} \sum_{i=1}^{N} \boldsymbol{f}_2^2(m_0, \eta) && (21)\\
m &\in [0,\ 2 \times m_{mtw}]\\
\eta &\in [0.8, 1]
\end{aligned}$$

Although the total energy equation is the same for descent flights, their thrust profiles are different. In the above equations, $\eta \cdot T_{max,i}$ needs to be replaced with idle thrust or appropriated descent thrust profile.

D. Inferring mass from breaking

Compared to takeoff, landing dynamics are more complicated. Spoilers are deployed to reduce lift, and breaks are applied at the same time, resulting in a higher friction coefficient μ_2. Both actions increase the ground drag. Sometimes, when a thrust reverser is available, reversed thrust (denoted by coefficient η_{rev}) is also deployed upon touch-down [12, P511]. Taking these aspects into consideration, aircraft mass can be approximated as follows:

$$m_i \approx \frac{-\eta_{rev} T_{idl} - 0.5 \rho V_i^2 S (C_{D0,ld} - \mu_2^2/(4K_{ld}))}{\mu_2 g + a_i} \tag{22}$$

$$\hat{m} = \frac{1}{N} \sum m_i \tag{23}$$

It is worth noting that these equations are very simplified estimations due to the large number of unknowns present during landing.

E. Fuel flow model

Mass estimations at any phase other than takeoff need to take into account the fuel flow in order to derive the aircraft initial mass. Two fuel flow models are available: the ICAO databank and the BADA3 fuel flow model.

1) ICAO fuel flow model: The ICAO engine emission databank defines fuel flow under four different modes: takeoff, climb-out, approach, and idle, with power settings at 100%, 85%, 30%, and 7% of engine maximum power respectively. It is important to note that data are all gathered from a static engine test. Hence, the fuel flow measurements are biased compared to dynamic flight data. Operational flight data and tests conducted by Zurich Airport [13] have shown that there is a difference between ICAO fuel flow model and operational fuel consumption.

In order to get the model closer to actual fuel consumption, based on the four points from the ICAO data bank, a quadratic fuel flow profile is constructed describing the fuel flow as a function of the fraction between actual thrust T and maximum static thrust T_∞, denoted as ϵ:

$$\dot{m}_{fuel} = K_1 \epsilon^2 + K_2 \epsilon + K_3 \tag{24}$$

From the ICAO data bank, fuel flow data are fitted with a polynomial model for several engines. Figure 2 shows the

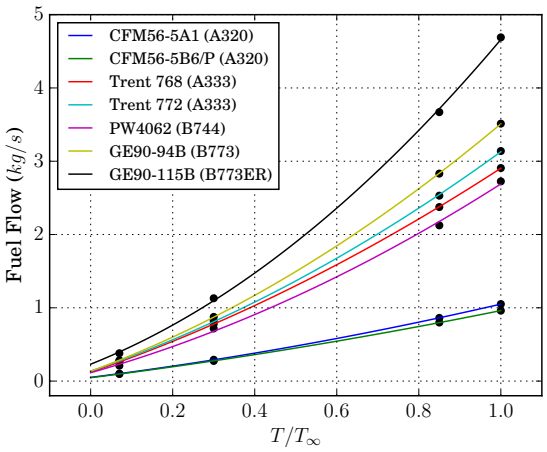

Fig. 2. ICAO Fuel Flow Interpolation

results of the fitted model obtained from data from several engines and their corresponding aircraft types.

For a common two-shaft turbofan engine it is possible to simplify the thrust model using an empirical relation between aircraft Mach number and pressure altitude [11]:

$$\epsilon = \frac{T}{T_\infty} = f_1(M, H) \tag{25}$$

Thus the actual fuel flow can also be calculated as a function f_2 of Mach number, altitude, and time obtained from the flight data. Finally, the consumed fuel mass can be integrated throughout the flight at any given time τ:

$$m_{fuel} = \int_0^\tau f_2(M, H, t)dt \tag{26}$$

2) BADA3 fuel flow model: The BADA3 calculation consists of three fuel flow modes, minimal (idle thrust at descent), cruise (cruise thrust), and nominal (other flight phases). With the BADA model, fuel flow can be calculated similarly to the previous method. It produces a relatively higher-accuracy result with more sophisticated models. Details of BADA fuel flow calculations can be found in the BADA user manual [8].

III. Bayesian Inference Method

Assume the aircraft mass is a univariate random variable follows a Normal distribution:

$$m \sim \mathcal{N}(\mu, \sigma^2) \tag{27}$$

Here, μ is the mean the this univariate Gaussian need to be estimated, whose variance is assumed as known variable. This fix variance assumption is to simplify following derivation.

Assuming n possible mass observations are obtained from different flight phases:

$$\boldsymbol{m} = m_1, m_2, \cdots, m_n \tag{28}$$

Those observations are possible values of initial aircraft mass. However, due to errors in aircraft flight data and estimations, those values can be very different from reality or even out of the physical boundaries.

The Bayesian inference method is based on the conditional probability theorem and is used to formulate a posterior probability model for certain parameters from observed data based on a prior probability distribution. In this case, it is used to estimate the probability of μ based on these n number of mass observations, denoted as $p(\mu|\boldsymbol{m})$.

A. Prior probability

The prior probability distribution (or simply prior) of a certain parameter expresses the belief of such parameter before any evidence (observations) is considered. It is usually based on empirical knowledge or values obtained from previous observations. For this paper, the prior represents the belief of the initial mass of aircraft m, which is bounded by its physical constraints (operational empty weight m_{oew} and maximum takeoff weight m_{mtw}) and likely close to a certain value μ_0 (for example, 80% of the maximum weight). It is also assumed a normal distribution with a variance of σ_0^2:

$$\mu \sim \mathcal{N}(\mu_0, \sigma_0^2) \tag{29}$$

B. Posterior probability

The posterior probability of an uncertain parameter is the conditional probability obtained after certain evidence (observations) are considered. It is calculated as follows:

$$p(\mu|\boldsymbol{m}) = \frac{\overbrace{p(\mu)}^{\text{Prior}} \cdot \overbrace{p(\boldsymbol{m}|\mu)}^{\text{Likelihood}}}{\underbrace{p(\boldsymbol{m})}_{\text{Scaling factor}}} \tag{30}$$

The estimate produced by Bayesian inference is known as the Maximum A Posteriori (MAP) estimate. Under the previously constant variance assumption, the MAP estimation of μ based on $\boldsymbol{m}$ can be derived in a simple closed-form easily.

First of all, the probability of all mass observations, also know as the the scaling factor $p(\boldsymbol{m})$, is the integration over all possible μ, which equals to $\int p(\mu)p(\boldsymbol{m}|\mu)d\mu$. Since the term $p(\boldsymbol{m})$ does not depend on the parameter μ with fixed $\boldsymbol{m}$, the posterior probability density $p(\mu|\boldsymbol{m})$ can be expressed as proportional to the multiplication of prior and likelihood, also called unnormalized posterior density, which is the right hand side of following equation:

$$p(\mu|\boldsymbol{m}) \propto p(\mu)p(\boldsymbol{m}|\mu) \tag{31}$$

The likelihood function $p(\boldsymbol{m}|\mu)$ is represented as the joint probability function of data. It is viewed as a function of the parameters and can be calculated as follows:

$$p(\boldsymbol{m}|\mu) = p(m_1, m_2, \ldots, m_n|\mu) = \prod_{i=1}^{n} p(m_i|\mu) \tag{32}$$

The remaining task is to calculate the posterior probability $p(\mu|\boldsymbol{m})$ based on the product of the prior probability and the likelihood.

1) Single observation case: Starting from a simple case, considering a single observation, its likelihood from the sampling distribution is:

$$\begin{aligned} p(m|\mu) &= \frac{1}{\sqrt{2\pi}\sigma} exp\left(-\frac{(m-\mu)^2}{2\sigma^2}\right) \\ &\propto exp\left(-\frac{(m-\mu)^2}{2\sigma^2}\right) \end{aligned} \tag{33}$$

and the distribution of the prior parameter μ is:

$$\begin{aligned} p(\mu) &= \frac{1}{\sqrt{2\pi}\sigma_0} exp\left(-\frac{(\mu-\mu_0)^2}{2\sigma_0^2}\right) \\ &\propto exp\left(-\frac{(\mu-\mu_0)^2}{2\sigma_0^2}\right) \end{aligned} \tag{34}$$

Then, the posterior distribution function for the single observation calculates as follows:

$$\begin{aligned} p(\mu|m) &\propto p(\mu)\ p(m|\mu) \\ &\propto exp\left(-\frac{(\mu-\mu_0)^2}{2\sigma_0^2} - \frac{(m-\mu)^2}{2\sigma^2}\right) \\ &\propto exp\left(-\frac{(\mu-\mu_1)^2}{2\sigma_1^2}\right) \end{aligned} \tag{35}$$

where:

$$\mu_1 = \frac{\sigma^2\mu_0 + \sigma_0^2 m}{\sigma^2 + \sigma_0^2} \quad \text{and} \quad \sigma_1^2 = \left(\frac{1}{\sigma_0^2} + \frac{1}{\sigma^2}\right)^{-1} \tag{36}$$

2) Multiple observation case: For multiple observations, the likelihood can be calculated similarly as follows:

$$\begin{aligned} p(\boldsymbol{m}|\mu) &= \prod_{i=1}^{n} p(m_i|\mu) \\ &\propto \prod_{i=1}^{n} exp\left(-\frac{(m_i-\mu)^2}{2\sigma^2}\right) \\ &\propto exp\left(-\frac{1}{2\sigma^2}\sum_{i=1}^{n}(m_i-\mu)^2\right) \\ &\propto exp\left(-\frac{1}{2\sigma^2}\sum_{i=1}^{n}(m_i^2 - 2m_i\mu + \mu^2)\right) \\ &\propto exp\left(-\frac{n}{2\sigma^2}(-2\bar{m}\mu + \mu^2)\right) \\ &\propto exp\left(-\frac{n}{2\sigma^2}(\bar{m}-\mu)^2\right) \\ &\propto p(\bar{m}|\mu) \end{aligned} \tag{37}$$

where $\bar{m} = (\sum m_i)/n$ represents the mean of all observations $\boldsymbol{m}$. The posterior probability then becomes:

$$\begin{aligned} p(\mu|\boldsymbol{m}) &\propto p(\mu)p(\boldsymbol{m}|\mu) \\ &\propto p(\mu)p(\bar{m}|\mu) \\ &\propto p(\mu|\bar{m}) \end{aligned} \tag{38}$$

Because m_i is considered of being drawn from a normal probability distributed function, the probability of $\bar{m}$ is also normally distributed with the variance of σ^2/n:

$$\bar{m} \sim \mathcal{N}(\mu, \sigma^2/n) \tag{39}$$

The relationship $p(\mu|\boldsymbol{m}) \propto p(\mu|\bar{m})$ in Equation 38 suggests the posterior probability of μ from multiple observations can be treated as a single observation, where the multiple observations $\boldsymbol{m}$ are substituted by the mean $\bar{m}$ (a sufficient statistic).

Combining the Equations 36 and 39, the posterior probability distribution of parameter μ based on multiple observations $\boldsymbol{m}$ can then be obtained in close form and described as follows.

Lemma 1: Assume independent and identically distributed random variables $m_i \sim \mathcal{N}(\mu, \sigma^2)$ given unknown μ, known σ, and $\mu \sim \mathcal{N}(\mu_0, \sigma_0^2)$. Then, from n number of observations $\boldsymbol{m} = [m_1, m_2, \cdots, m_n]$, the posterior probability distribution of μ satisfies the following normal distribution:

$$\mu|\boldsymbol{m} \sim \mathcal{N}\left(\frac{n\sigma_0^2\bar{m} + \sigma^2\mu_0}{\sigma^2 + n\sigma_0^2}, \quad \left(\frac{1}{\sigma_0^2} + \frac{n}{\sigma^2}\right)^{-1}\right) \tag{40}$$

Figure 3 illustrates an example of a MAP estimate of aircraft initial mass based on the prior distribution and five independent initial mass measurements from different flight phases.

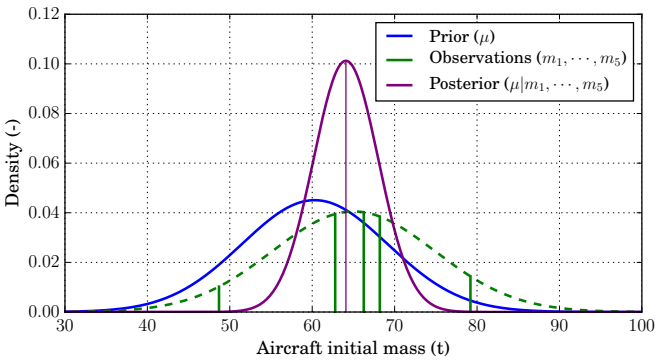

Fig. 3. Example of Bayesian inference

It is possible to see that the maximum a posteriori estimate is slightly biased towards the prior in comparison to the mean of measurements. This aspect will be addressed in the later discussion section.

IV. Experiments and results

To examine and validate the Bayesian estimation approach, data of thousands of flights from four different aircraft types are gathered. The dataset consists of around 1500 flights for each aircraft type. For each flight, five initial mass measurements are computed at different flight phases using the respective methods. After that, the Bayesian mass inference is applied. Three sets of results are presented. The first focuses on one particular aircraft type, the Airbus A320. The second includes the inference statistics of all four aircraft types. Finally, the parameter sensitivities are shown.

A. Results of a single aircraft type

The results for the Airbus A320 are shown in Figure 4. The first five sub-plots illustrate the distribution of individual measurement results from methods that are applied at different flight phases, which are takeoff, liftoff, climb, descent, and final approach. The last plot shows the final estimated initial masses using Bayesian inference.

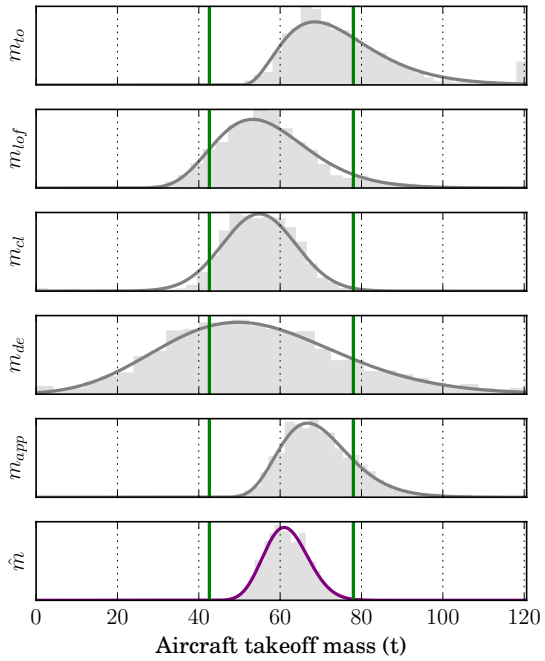

Fig. 4. Comparison of estimations at different flight phases (A320, 1500 flights)

For the distributions of the measurements and final inferences, it is evident that the MAP estimates have a smaller variance than the individual estimates, and most of the initial estimates are within the boundaries of m_{oew} and m_{mtw}. It is also worth noting that the prior chosen for this experiment is a relatively weak prior, so the result are less biased.

For each flight, based on all individual observations, the means and standard deviations are also computed and compared against the MAP estimation, shown in Figure 5. In the first plot, the statistical difference in estimated μ is not very large. This is due to the weak prior used in the Bayesian estimation. Regardless, under the Bayesian inference, both the minimum and maximum of all estimations fall in the boundary of possible Initial mass, and there are significantly fewer outliers in the outcome. The uncertainty of the estimation can also be obtained, as shown in the the second plot, where the Bayesian inference provides a lower uncertainty in general.

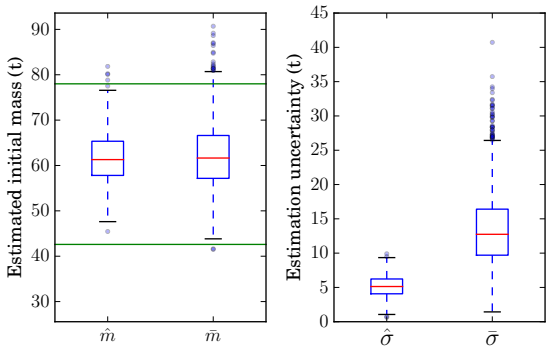

Fig. 5. Performance of Bayesian inference (A320, 1500 flights)

B. Multiple aircraft types

The same inference methods are applied to different aircraft types. The results of these estimations are shown in Figure 6. For each aircraft type, around 1500 complete flights are analyzed. Within each plot, two green dash lines mark the possible initial mass boundary that is constrained by m_{oew} and m_{mtw}, where the unit of mass is metric ton (t). The horizontal axis in each figure represents the mass computed at takeoff, lift-off moment, climb, descent, and approach, with final inferred mass.

Comparing these four different aircraft types, it is possible to conclude that at different flight phases the calculated initial mass tends to be biased towards the same end, some of which contain very inaccurate estimates. However, the Bayesian inference is able to produce an estimation that is able to overcome these extremes and produce reasonable estimates. The cause for these biases are addressed in the discussion section.

C. Parameter sensitivities

1) Thrust settings: The level of correctness of aircraft mass estimations based on observed performance parameters is essentially dependent on knowledge of thrust settings. As shown in Section II, most of the mass computation methods along the flight path need to take into account the thrust profile while estimating aircraft mass. In these methods, an optimization using the least squares method is implemented to find the best thrust setting and aircraft mass, which provides a minimal squared error. This approach has also been proposed previously by Alligier et al. [2] This approach makes sense mathematically. However, without validation using measured thrust data, it is not possible to conclude whether the thrust configuration obtained for the optimization is indeed the correct setting.

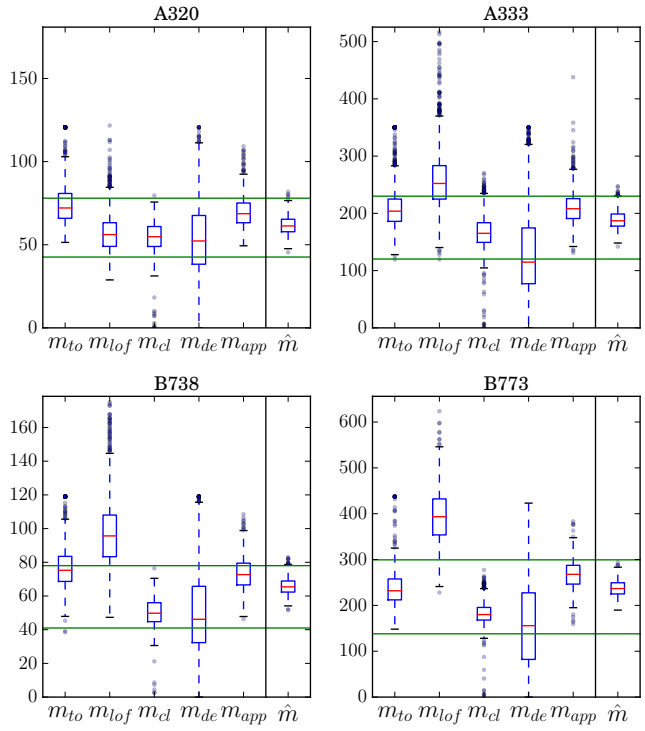

Fig. 6. Initial mass estimation of four aircraft types

Other sources of errors in the observed performance parameters are the observations of positions, altitudes, velocities, and climb/descent rates, which are obtained from ground stations, either in the format of ADS-B (this paper) or from surveillance radar data.

In order to study the influence of different thrust settings, based on the same dataset, two fixed minimum and maximum thrust profiles are used to produce two different sets of mass estimates. For takeoff and climb, maximum thrust and a 30% reduced thrust profile are used. While for descent, two thrust settings at 8% and 20% of maximum climbing thrust setting are used. In Figure 7, results from such different settings are computed and compared.

During the takeoff and climb, higher thrust settings lead to higher estimations of initial masses, and this difference is statistically significant. During the descent phase, such a tendency is not visible. However, the uncertainty of mass is much larger compared to other two flight phases. The final initial mass estimate produced by Bayesian inference is still within the possible boundaries, but with considerable differences. From these results, it is obvious that thrust setting is a significant factor that affects the mass estimation in general.

2) Airspeed vs ground speed: All estimation methods introduced in Section II require correct measurements of aircraft true speed. However, data collected from ground measurements (ADS-B or radar) only reveal the ground speed. Estimations can either assume the ground speed as airspeed or integrate wind data to approximate the airspeed. Intuitively, this uncertainty in wind can affect the estimation results.

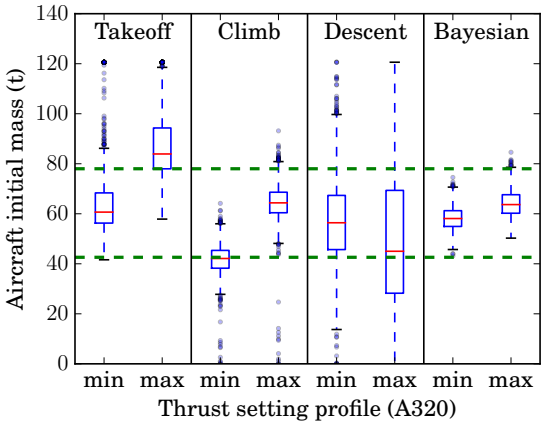

Fig. 7. Sensitivity on thrust settings

In the experiment dataset, meteorological data are integrated with ADS-B ground speed to approximate the true airspeed of aircraft [14]. Climb with maximum thrust profile and an idle thrust descent profile are considered. For each flight, initial mass is computed with both ground speed and approximated airspeed. In Figure 8, the distributions of these differences in climb, descent, and final estimation are shown. From the third plot, it can be seen that depending on the level of the wind speed, the estimation can vary up to five metric tons of difference for the Airbus A320. This can be up to 8% of the nominal weight according to previous results shown in Figure 4.

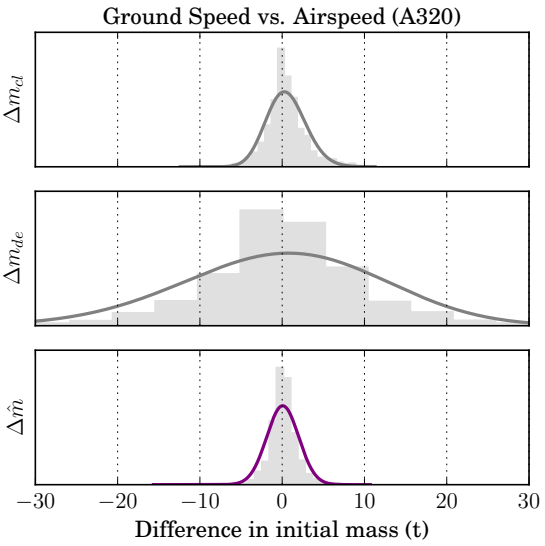

Fig. 8. Difference in estimation caused by wind

However, this difference can not be shown statistically by observing all flights in the dataset as shown in Figure 9. This is because for a large number of flights, the effect of wind averages out.

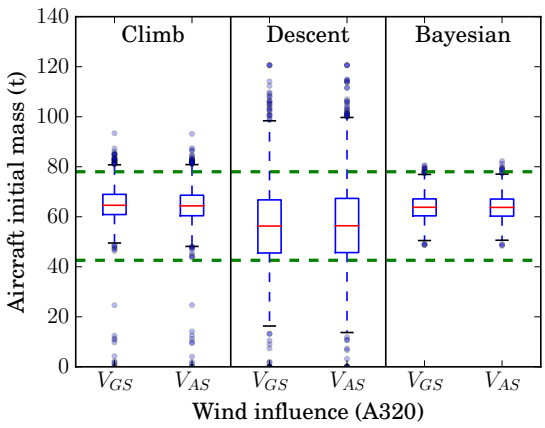

Fig. 9. Estimation sensitivity on wind

3) Prior distribution: When applying Bayesian inference, one of the important factors is the prior. Stronger belief in the prior knowledge will increase the confidence of the final estimation. However, these estimates can be biased toward prior belief. To study this influence, the same dataset is used with a set of different priors to produce estimates from Bayesian inference. In Figure 10, six combinations of (μ_0, σ_0) are chosen to study this effect. The probability distribution functions that are biased towards low, medium, and high mass are shown in red, black, and blue, respectively. Priors with high and low confidence are shown in solid and dashed lines, respectively.

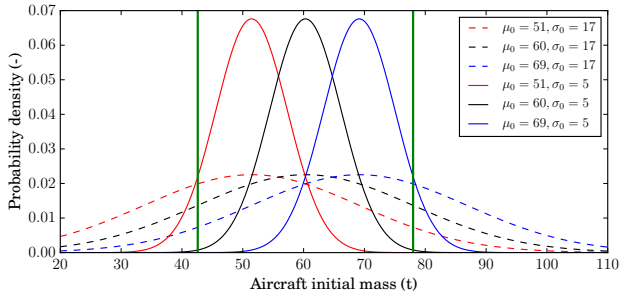

Fig. 10. Different initial mass prior distribution (A320)

In Figure 11, six different results from the same estimation configuration are displayed. On the left side are plots where low confident priors (large σ_0) with different μ_0 are applied, while on the right side are results form high confident priors (low σ_0).

From those plots, it is possible to understand that with a weak prior, the estimates are less biased. They depend more on the observations (i.e.: different initial mass calculated at different flight phases). This will also produce less confident results, i.e., all three experiments end up with estimates with larger variance.

When the level of belief is increased, the estimations start to follow this prior distribution. This produces more confidence

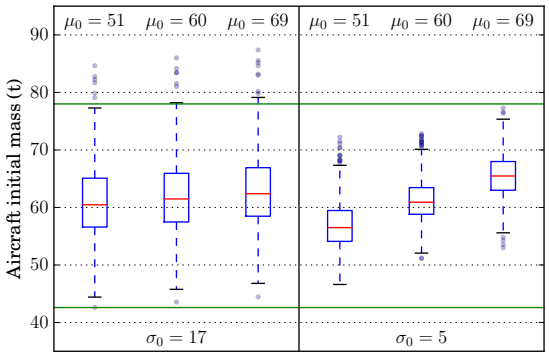

Fig. 11. Estimation sensitivity on prior distribution (A320)

but also biases estimates as shown on the right-hand side of the plots.

Hence, in addition to acquiring more accurate data to improve the accuracy of the observation, it is important to select a proper prior in this Bayesian inference process in order to produce realistic estimation.

V. Discussion

A. MAP vs MLE estimations

Fig. 5 shows how the maximum a posteriori estimation (MAP) approach compares to the maximum likelihood estimation (MLE) approach. For a normally distributed PDF, the MLE returns the estimate as the mean of the observations. MAP is the Bayesian approach that is based on the conditional probability theory where a certain prior (or "belief") of the parameter is known. This tends to lead the estimate bias to what the "belief" is. If the belief is strong and correct, the MAP tends to yield a better estimate. However, if the belief is strong but incorrect, the MAP estimates will be worse than MLE estimates. In practice, other than the minimum and maximum allowed weight, one can construct the prior based on direct or indirect indicators such as historical data, occupancy rate, and fuel reserves.

A normally distributed prior on initial mass is assumed in this paper. This assumption is based on results of previous studies [2] [15]. Furthermore, it also serves the purpose of simplifying the computation. Nonetheless, different types of parameter distributions can also be used.

B. Incomplete data and partial trajectory

In this paper, each flight in the dataset contains the complete flight trajectory data that starts before takeoff and lasts until landing is completed. It may include some missed segments during cross-ocean cruise where no data is available. The completeness of trajectory data is required to demonstrate all different mass calculation methods at each flight phase. However, such a condition is not required in order to arrive at a set of estimates. A partial trajectory can be used in the same way, where the number of measurements is simply reduced.

When dealing with partial trajectories or making real-time inference, the climb and descent phases can be segmented

further to create multiple measurements at different flight levels. The same method in Equation 21 can be applied to obtain more observations for applying the Bayesian inference process.

C. Individual methods bias

From Fig. 6, it is apparent that certain measurements tend to be biased and/or have large variances, especially the measurements at the liftoff moment and during descent phase.

For the liftoff moment, referring to Equation 12, the mass is calculated under the assumption of a 20% speed margin. It is possible that in reality for certain aircraft this margin is higher.

During the descent, the situation is more complicated than during the climb. Aircraft trajectories are more subjected to procedures from air traffic controllers. Additionally, different types of continuous descent approaches maybe used. Thus, the thrust settings can substantially differ among flights. Optimization according to Equation 21 may not yield the best thrust-mass setting to resemble reality. This effect can be seen in Figure 7 in the descent phase. One possible solution is to reduce the thrust setting range towards idle thrust, but doing so may cause those higher powered descents to suffer a biased result. A better way to approach this is to identify the type of descent approach (traditional profile or CDA profile), then assign different thrust setting boundaries accordingly. This can be implemented in future studies.

D. Reduced thrust takeoff and climb

Using the total energy model in Equation 1, with observed aircraft kinematic states and calculated drag, there are multiple possible thrust and mass combinations. That is, both higher and lower thrust-mass combinations may satisfy the equation at the same time.

It is fairly common for aircraft to perform reduced thrust takeoff and climb. Several estimation methods used in this paper require knowledge of the ratio of reduced thrust. That is also the reason for using the least squares optimization method in Equation 21. It tries to find the best combination of thrust setting and mass. This approach is similar to previous research [2]. However, without aircraft on-board data as validation, this remains to be a large source of uncertainties in the domain of aircraft mass estimations.

VI. Conclusions

A Bayesian inference method to estimate aircraft initial mass has been proposed in this paper. As input for the Bayesian inference, different ways for computing aircraft mass based on trajectory data are summarized. In combination with a simplified fuel flow model from the ICAO data bank, different measurements of aircraft initial mass at takeoff are generated. The Bayesian inference process can obtain improved estimates based on certain prior knowledge of the probability distribution of the aircraft mass. Parameter sensitivity studies are also carried out to test the robustness of the method. Compared to previous studies, this method is able to provide a reasonable estimate and a level of confidence on any given trajectory, as long as the aircraft type is known.

References

[1] Sun, J., Ellerbroek, J., and Hoekstra, J., "Modeling and Inferring Aircraft Takeoff Mass from Runway ADS-B Data," *7th International Conference on Research in Air Transportation*, 2016.

[2] Alligier, R., Gianazza, D., and Durand, N., "Learning the aircraft mass and thrust to improve the ground-based trajectory prediction of climbing flights," *Transportation Research Part C: Emerging Technologies*, Vol. 36, nov 2013, pp. 45–60.

[3] Alligier, R., Gianazza, D., and Durand, N., "Machine learning and mass estimation methods for ground-based aircraft climb prediction," *IEEE Transactions on Intelligent Transportation Systems*, Vol. 16, No. 6, 2015, pp. 3138–3149.

[4] Schultz, C., Thipphavong, D., and Erzberger, H., "Adaptive trajectory prediction algorithm for climbing flights," *AIAA Guidance, Navigation, and Control (GNC) Conference*, 2012, p. 2.

[5] Lee, H.-t. and Chatterji, G., "Closed-Form Takeoff Weight Estimation Model for Air Transportation Simulation," *10th AIAA Aviation, Technology, Integration, and . . . , pages = 1–13, year = 2010*.

[6] Chatterji, G. B., "Fuel burn estimation using real track data," *11th AIAA ATIO Conference*, 2011.

[7] Chati, Y. S. and Balakrishnan, H., "Statistical Modeling of Aircraft Engine Fuel Flow Rate," *30th Congress of the International Council of the Aeronautical Science*, 2016.

[8] Nuic, A., "User manual for the Base of Aircraft Data (BADA) revision 3.12," *Atmosphere*, Vol. 2014, 2014.

[9] ICAO, "Aircraft Engine Emissions Databank," 2016.

[10] Wetmore, J., "The Rolling Friction of Several Airplane Wheels and Tires and the Effect of Rolling Friction on Take-Off," 1937.

[11] Bartel, M. and Young, T. M., "Simplified Thrust and Fuel Consumption Models for Modern Two-Shaft Turbofan Engines," *Journal of Aircraft*, Vol. 45, No. 4, 2008, pp. 1450–1456.

[12] Obert, E., *Aerodynamic design of transport aircraft*, Ios Press, 2009.

[13] Fleuti, E. and Polymeris, J., "Aircraft NOx-Emissions within the Operational LTO Cycle," Tech. rep., Flughafen Zurich AG, 2004.

[14] Sun, J., Ellerbroek, J., and Hoekstra, J., "Large-Scale Flight Phase Identification from ADS-B Data Using Machine Learning Methods," *7th International Conference on Research in Air Transportation*, 2016.

[15] Alligier, R., Gianazza, D., Ghasemi Hamed, M., and Durand, N., "Comparison of Two Ground-based Mass Estimation Methods on Real Data," *6th International Conference on Research in Air Transportation (ICRAT)*, 2014, pp. 1–8.

Authors' Biographies

Junzi Sun is a Ph.D. candidate at the Delft University of Technology. He received his M.Sc from the Polytechnic University of Catalonia. His doctoral research topic is aircraft performance modeling using open flight data, with focuses on machine learning, data mining, modeling, and statistical inferences.

Joost Ellerbroek received the M.Sc. and Ph.D. degrees in aerospace engineering from the Delft University of Technology, The Netherlands, in 2007 and 2013, respectively. His research interests are in the domain of air-traffic management, including analysis of airspace complexity, and the design and analysis of conflict detection and resolution algorithms.

Jacco M. Hoekstra is a full professor at the faculty of Aerospace Engineering of the Delft University of Technology. After obtaining his M.Sc. and pilots license in 1990, he started working at the National Aerospace Laboratory (NLR). He then obtained his Ph.D. on Air Traffic Management and headed the NLR Air Transport Operations division, before joining the TU Delft faculty. He served two terms as a dean and now heads the CNS/ATM chair.